SUPPLEMENTAL MATERIALS for Golebiewska et al. "Evidence for a fence that impedes the diffusion of phosphatidylinositol 4,5-*bis*phosphate (PIP_2) out of the forming phagosomes of macrophages"

Section 1. The level of PIP_2 in the forming phagosomes of J774 macrophages first increases, then decreases, as was previously observed in RAW macrophages.

Figure S1A suggest PIP_3 also increases in the cup. Figure S1B shows that the fluorescence due to a GFP-tagged PH domain from PLCδ1 (PH-PLCδ-GFP) is enhanced during early stages of the forming phagosome; Figure S1C shows the fluorescence decreases later. The caveats in interpreting a change in the concentration of PH-PLCδ-GFP in terms of a change in the concentration of PIP_2 are discussed elsewhere (Balla et al., 2000; Watt et al., 2002; Varnai et al. 2002; Balla, 2010). Field et al. (2005) made the important observation that a similar increase in the concentration of PIP_2 in the furrows beween cells was observed using either tagged TUBBY or the PH domain of PLCδ1. A recent report from the Hille laboratory discusses the kinetics of the metabolism of PIP_2 in cells (Falkenburger et al., 2010).

Section 2. FRAP control measurements with DiI within the cup and PIP_2 outside the cup; the advantages of FCS vs FRAP measurements for determining the diffusion coefficients of lipids; FCS and FRAP measurements on PM-GFP.

The fluorescence due to the lipid DiI fully recovers after FRAP of the forming phagosome region. There is essentially a full recovery of fluorescence when DiI-C12 is bleached in the forming phagosome. This is expected because DiI flip-flops rapidly across the plasma membrane and the available evidence suggests there is no fence or barrier to diffusion on the outer leaflet (see section 3 below). Thus, the experiment is essentially a control to show that the lack of recovery in the forming phagosome noted with fluorescent PIP_2 (Figure 3) and PM-GFP (Figures 4, S3) is not due to a technical difficulty in measuring recovery in the vicinity of the bead.

The fluorescence due to TopFluor PIP_2 recovers fully and rapidly after photobleaching an area of radius ~3 μm outside the region of the forming phagosome in J774 macrophages. We observed a rapid (half time for recovery ~10 s) essentially complete (95 % ± 15% SD, n = 6) recovery of the fluorescence due to TopFluor PIP_2 when we bleached an area of radius ~3 μm in an unstimulated J774 macrophage (see Figure 3E for one example). We considered the recovery to be 100% if the fluorescence in the bleached area returned to the average level of fluorescence in the cell membrane outside the area of bleach after 100 s. This level did decrease significantly from the initial level. The result is qualitatively different from the behavior observed within the cup (Figure 3D), where the fluorescence did not recover substantially in 100 s. Thus, similar results are obtained with both fluorescent PIP_2 and PM-GFP (Figures 3E, 4, S3) when we bleach an area outside the cup: rapid, essentially complete recovery that is

consistent with free diffusion of both the lipid and GFP-tagged plasma membrane anchored peptide.

Advantages of using FCS vs FRAP to monitor D of PIP_2 and PM-GFP in the plasma membrane of living cells. As discussed in detail elsewhere (Chen et al. (2006); Guo et al. (2008)), essentially identical results are obtained using either FCS or FRAP to measure the D of a lipid in a model phospholipid membrane. There are two main advantages to using FCS to measure the diffusion constant, D, of a lipid in a biological membrane. *First*, FCS measurements require only a very low concentration of fluorescently tagged lipid molecules, which do not significantly alter the level of endogenous lipid (e.g., PIP_2). Specifically, in our experiments shown in Figure 2 the confocal area of radius 0.22 μm contains about 10^5 phospholipids, 10^3 PIP_2 and 10 fluorescently tagged PIP_2. In contrast, our FRAP measurements (e.g., Figure 3) require ~ 100-fold higher surface concentrations of PIP_2, which may perturb the level of endogenous PIP_2. Furthermore, one needs to use higher pressures, longer injection times to inject this additional PIP_2. *Second*, the spatial resolution is superior for FCS measurements. FCS data are collected from a small area, of radius 0. 2 – 0.3 μm for a typical confocal microscope; smaller for a STED-FCS apparatus (Eggerling et al. 2010). For FRAP measurements, a larger area is required. We also note that a powerful laser is required to bleach a 1 μm radius spot sufficiently rapidly (in << 0.1 s, the time it takes a typical lipid to diffuse this distance) to make accurate FRAP determinations of D. Thus, even with a 4 μm radius spot, a 1 s bleach time will bleach a significant number of molecules outside the spot that diffuse in during the bleach time, and a significant number of bleached molecules will diffuse out of the spot. We regard our FRAP measurements merely as qualitative estimates of the ability of PM-GFP and PIP_2 to diffuse in the membrane. (Specifically, we anticipate that the time constant in our FRAP measurements of PM-GFP and PIP_2 will underestimate the correct D of these molecules in the membrane. The D we estimate from FRAP measurements is indeed lower than the D from FCS.) Fortunately, more sophisticated FRAP measurements (Hammond et al., 2009) using PM-YFP in HEK cells yields a value for D (0.79 $\mu m^2/s$) that is the same, within experimental error, to the value we obtained from FCS measurements for PM-GFP in macrophages (0.9 ± 0.5 $\mu m^2/s$ (n = 25 ± SD), see Results). There are other caveats: the membrane at the base of the cup may be remodeled during the measurement, due to insertion of new membrane through exocytosis.

FCS and FRAP measurements on PM-GFP. FCS measurements on PM-GFP and PMT-GFP were described with a two-component fit; one corresponding to diffusion within the membrane and one with a much shorter (~100-fold) correlation time, which minimally composed 30 % of the sampled population of fluorescent molecules for both PM-GFP and PMT-GFP expressed in RAW macrophages. The correlation time of the more rapidly diffusing species corresponded to that expected for GFP diffusion within the cytoplasm. One interpretation is that a subpopulation of PM-GFP molecules fail to be both myristoylated and palmitoylated. As the correlation time of the rapidly diffusing species is 100-fold faster than the correlation time of interest (i.e. membrane diffusion), we disregarded this component. The correlation times we obtained for membrane diffusion were independent of the proportion of fluorescence from the cytosolic fraction.

Figure. S3 shows additional FRAP measurements that complement the results shown in Figure 4. In this protocol we bleached only the base of the cup, then examined recovery in this region. See Figure S3, left panel, Cup. The region indicated by the white ellipse was bleached, and the recovery followed in this area is indicated by the red curve in B. The right hand panel under Cup shows the transmitted light images, indicating the position of the engaged IgG-coated 8 μm bead. The right hand two panels (under PM label) show a subsequent bleach of an approximately equal area of plasma membrane outside the cup region on the same cell. Note the recovery after 75 and 150 seconds. When we prebleached this area outside the cup the recovery is essentially complete, as shown in the green curve in part B. One interpretation of this result is that ~ 100% of the PM-GFP in the plasma membrane is free to diffuse but that ~30% of the PM-GFP is located on endomembranes beneath the plasma membrane. A second interpretation is that ~30% of the PM-GFP is free in the cytoplasm, as suggested by the FCS measurements, and is bleached during the prebleach. A third interpretation is that 30% of the PM-GFP in the plasma membrane is truly immobile.

We reasoned that the bleach protocol in Figure 4 (bleach cup, follow recovery in cup) or Figure S3 (bleach base of cup, follow recovery in base of cup), should produce a partial rather than a full recovery, even if there was a fence at the perimeter or lip of the cup or forming phagosome. In the first case, PM-GFP should diffuse from the bulk plasma membrane into the edges of the cup; in the second case from the unbleached edge into the bleached base. We reasoned that bleaching the entire cup and examining just the base should reduce recovery to zero if a fence truly blocked entry of PM-GFP into the base. However, when we performed this bleach sequence we again observed about 20% recovery (not shown). The result may be due to technical difficulties or to addition of new membrane to the base area.

Section 3. A reinterpretation of the Corbett-Nelson et al. (2006) data obtained with PM-GFP in macrophages.

Plasma-membrane-anchored GFP molecules are widely used in cell biology as membrane markers. A plasma-membrane-targeted GFP based on the first 10 residues of the Src family kinase Lyn (which is presumably myristoylated cotranslationally on the N terminal glycine residue and palmitoylated on the cysteine residue) was used to study phagocytosis in macrophages by Corbett-Nelson et al. (2006). This construct was termed PM-GFP in their report and Lyn-GFP in other reports. Although the data that they obtained and the data we report here are qualitatively in accord, we re-interpret several of their conclusions in the light of our current results. First, although the recovery times from their FRAP measurements of PM-GFP and lipids were similar to those reported here (~ 10 s) they calculated an order of magnitude slower diffusion coefficient than we do. The obvious problem is the assumption one can bleach only the PM-GFP molecules in a small illuminated spot of radius 1 μm by illuminating for ~2s. The Einstein relation shows that if the diffusion coefficient is actually of order 1 $\mu m^2/s$, molecules from a ~3-fold larger radius will diffuse into the illuminated area and be bleached during the 2 s exposure to intense laser light. Underestimating the effective

radius of the bleached spot by ~3-fold leads to a ~10-fold error in the calculated value of D. We determined the diffusion coefficient, D, from independent FCS and FRAP measurements and regard the D determined from FCS measurements as more reliable as noted in Section 2 above. We deduce a value of D ~ 1 $\mu m^2/s$ for the diffusion coefficient of PM-GFP both inside and outside the cup region from these FCS measurements. This is very similar to the value we deduce for the lipid PIP_2 (D ~ 1 $\mu m^2/s$). It agrees qualitatively with the FCS measurements of Liu et al (2007) using a similar myristolyated/ palmitoylated plasma membrane targeted GFP, PMT-GFP, which we also investigated on the RAW macrophages (we obtained similar FCS data with both PMT-GFP and PM-GFP).

The second difference in interpretation relates to the fraction of fluorescence recovery after bleach of PM-GFP. Both Corbett-Nelson et al. (2006) and we (Figure S4) observe essentially a full recovery when bleaching PM-GFP in the region outside the cup. We both observe a lack of full recovery when PM-GFP is partially bleached in the cup. They suggested the lack of recovery was due to an immobile fraction of ~ 50% of the GFP-PM in the cup. We now interpret the measurements to mean *not* that there is an immobile fraction in the cup region, but that a 'fence' limits the diffusion of PM-GFP into the bleached area of the cup. Specifically, the mobile fraction should not depend on the area bleached. Under their conditions (bleaching a small area for ~ 2s), the immobile fraction appeared to be ~50%. However, when we bleached a larger area of the forming phagosome, and thus a larger fraction of PM-GFP in the cup, it is apparent that a larger fraction of the fluorescence does not recover (e.g. Figure 4, Figure S3). A parsimonious interpretation of these results is that a fence limits diffusion of the unbleached PM-GFP into the forming phagosome.

Third, Corbett-Nelson et al. (2006) observed that GPI-GFP (or YFP), which are localized to the outer monolayer of the plasma membrane, fully recovers from bleach both within and outside the cup. The simplest interpretation of these results is that no fence limits the diffusion of these membrane-anchored proteins on the outer leaflet of the forming phagosome. The fence observed in this report for PIP_2 and PM-GFP apparently only affects molecules diffusing on the inner leaflet of the macrophage plasma membrane.

Finally, Corbett-Nelson et al. (2006) observed that Src family kinase inhibitor PP1, which is known to inhibit phosphorylation of the Fcγ receptor and prevent internalization of the particles, also allowed full recovery of PM-GFP fluorescence in the cup after bleaching. Although additional experiments are required, this result is consistent with the hypothesis that phosphorylation of the Fcγ receptor is required for formation of the fence on the inner leaflet.

Section 4. Langevin dynamics (LD)/electrostatic calculations on actin filaments close to membranes suggest actin filaments do not act as PIP_2 fences (Figure S4).

Section 5. The human septin filament has a positively charged face.

As discussed by McMurray & Thorner (2009) “Mechanistically, how septins create a barrier to diffusion along a membrane remains largely unknown.” They correctly noted that “protein-membrane interaction is often mediated by motifs in the protein that contain multiple basic residues that can interact electrostatically with the negatively charged head groups of phosphoinositides and/or other acidic glycerophospholipids.” Although the structure of the hetro-hexamer unit of mammalian septin filaments is known (Sirajuddin et al. 2007), the electrostatic potential adjacent to this unit has not been reported.

We performed such electrostatic calculations (150 mM salt, using the approach outlined in Jo et al. (2008)), which are shown in Figure S5. These calculations identify a positively charged (blue) or basic face of the septin hexamer, and thus of the filament. The membrane-binding cluster of 4 basic residues in the N terminus of many septins, a cluster previously identified from mutational studies (Zhang et al., 1999), is located on this face. Figure S5, in conjunction with previous theoretical and experimental work on other proteins (e.g. Src, K-ras, MARCKS, Bar-domain containing proteins) suggests the positively charged face of the septin hexamer will bind strongly (> 10 kcal/mol) to the negatively charged inner leaflet of the plasma membrane through electrostatic interactions (McLaughlin and Murray, 2005). Importantly, Bertin et al. (2010) showed incorporating PIP_2 into a monolayer greatly enhances the binding of budding yeast septin octamers. Thus, electrostatic interactions with acidic lipids such as PS and PIP_2 could suffice to anchor the septin octamers/hexamers and thus the septin filament to the inner leaflet. Other interactions (e.g. penetration of hydrophobic residues on the basic face into the membrane; coiled coil interactions between the C terminal extensions; specific interactions with other proteins) are almost certain to also occur.

References for Supplemental Materials

Balla T. (2010). Putting G protein-coupled receptor-mediated activation of phospholipase C in the limelight. J. Gen. Physiol. *135*, 77-80.

Balla T., Bondeva T., and Varnai P. (2000). How accurately can we image inositol lipids in living cells? Trends Pharmacol. Sci*. 21*, 238–41.

Bertin, A., McMurray, M.A., Thai, L., Garcia, G., Votin, V., Grob, P., Allyn, T., Thorner, J., Nogales, E. (2010). Phosphatidylinositol-4,5-*bis*phosphate promotes budding yeast septin filament assembly and organization. J. Mol. Biol. *404*, 711-731.

Chen, Y., Lagerholm, B. C., Yang, B., and Jacobson, K. (2006). Methods to measure the lateral diffusion of membrane lipids and proteins. *Methods* 39, 147-153

Corbett-Nelson, E. F., Mason, D., Marshall, J. G., Collette, Y. and Grinstein, S. (2006). Signaling-dependent immobilization of acylated proteins in the inner monolayer of the plasma membrane. J Cell Biol. *174*, 255-265.

Eggeling, C. Ringemann, C., Medda, R., Schwarzmann, G., Sandhoff, K., Polyakova, S., Belov, V. N., Hein, B., von Middendorff, C., Schonle, A., and Hell, S. W. (2010). Direct observation of the nanoscale dynamics of membrane lipids in a living cell. Nature 457, 1159-1163.

Falkenburger, B.H., Jensen, J.B., and Hille, B. (2010). Kinetics of PIP_2 metabolism and KCNQ2/3 channel regulation studied with a voltage sensitive phosphatase in living cells. J. Gen. Physiol. *135*, 99-114.

Field, S. J., Madson, N., Kerr, M. L., Galbraith, K. A. A., Kennedy, C. E., Tahiliani, M., Wilkins, A., and Cantley, L.C. (2005). PtdIns(4,5)P2 functions at the cleavage furrow during cytokinesis. *Current Biol.* 15, 1407-1412.

Guo, L., Har, J.Y., Sankaran, J., Hong, Y., Kannan, B. and Wohland, T. (2008) Molecular diffusion measurements in lipid bilayers over wide concentration ranges: a comparative study. Chem Phys Chem *9*, 721-728.

Hammond, G.R.V., Sim, Y., Lagnado, L., and Irvine, R.F. (2009). Reversible binding and rapid diffusion of proteins in complex with inositol lipids serves to coordinate free movement with spatial information. J. Cell Biol. *184*, 297-308.

Jo, S., Vargyas, M., Vasko-Szedlar, J., Roux, B., and Im, W. (2008). PBEQ-solver for online visualization of electrostatic potential of biomolecules. Nucl. Acids Res. *36*:W270-275.

Liu, P. Sudhaharan, T., Koh, R. M. L., Hwang, L. C.Ahmed, S., I. N. Maruyama, Wohland, T. (2007). Investigation of the dimerization of proteins from the epidermal growth factor receptor family by single wavelength fluorescence cross-correlatoin spectroscopy. Biophys. J*. 93*, 684-698.

McLaughlin, S., and Murray, D. (2005). Plasma membrane phosphoinositide organization by membrane electrostatics*.* Nature *438*, 605-611.

McMurray, M.A., and Thorner, J. (2009). Septins: molecular partitioning and the generation of cellular asymmetry. Cell Division *4*:18

Scott, C. C. Dobson, W., Botelho, R. J., Coady-Osberg, N., Chavrier, P., Knecht, D. A., Heath, C., Stahl, P., and Grinstein, S. (2005). Phosphatidylinositol-4,5-bisphosphate hydrolysis directs actin remodeling during phagocytosis. J. Cell Biol*. 169,* 139-149.

Sirajuddin, M., Farkosovsky, M., Hauer, F., Kuhlmann, D., Macara, I. G., Weyland, M., Stark, H. and Wittinghofer, A. (2007). Structural insight into filament formation by mammalian septins. Nature *449*, 311-315

Varnai, P. Lin, X., Lee, S. B., Tuymetova, G., Bondeva, T., Spat, A., Rhee, S. G., Hajnoczky, G., and Balla, T. (2002). Inositol lipid binding and membrane localization of

isolated pleckstrin homology (PH) domains. Studies on the PH domains of phospholipase C δ_1 and p130. J. Biol. Chem. *277*, 27412-27422.

Watt, S. A. Kular, G. Fleming, I. N., Downes, C. P., and Lucocq, J. M. (2002). Subcellular localization of phosphatidylinositol 4,5-bisphosphate using the pleckstrin homology domain of phospholipase C delta 1. Biochem. J*. 363*: 651-665.

Zhang J., Kong, C., Xie, H., McPherson, P. S., Grinstein, S., and Trimble, W. S. (1999). Phosphatidylinositol polyphosphate binding to the mammalian septin H5 is modulated by GTP. Current Biol. *9*, 1458-1467.

Figures and legends for Supplemental Materials

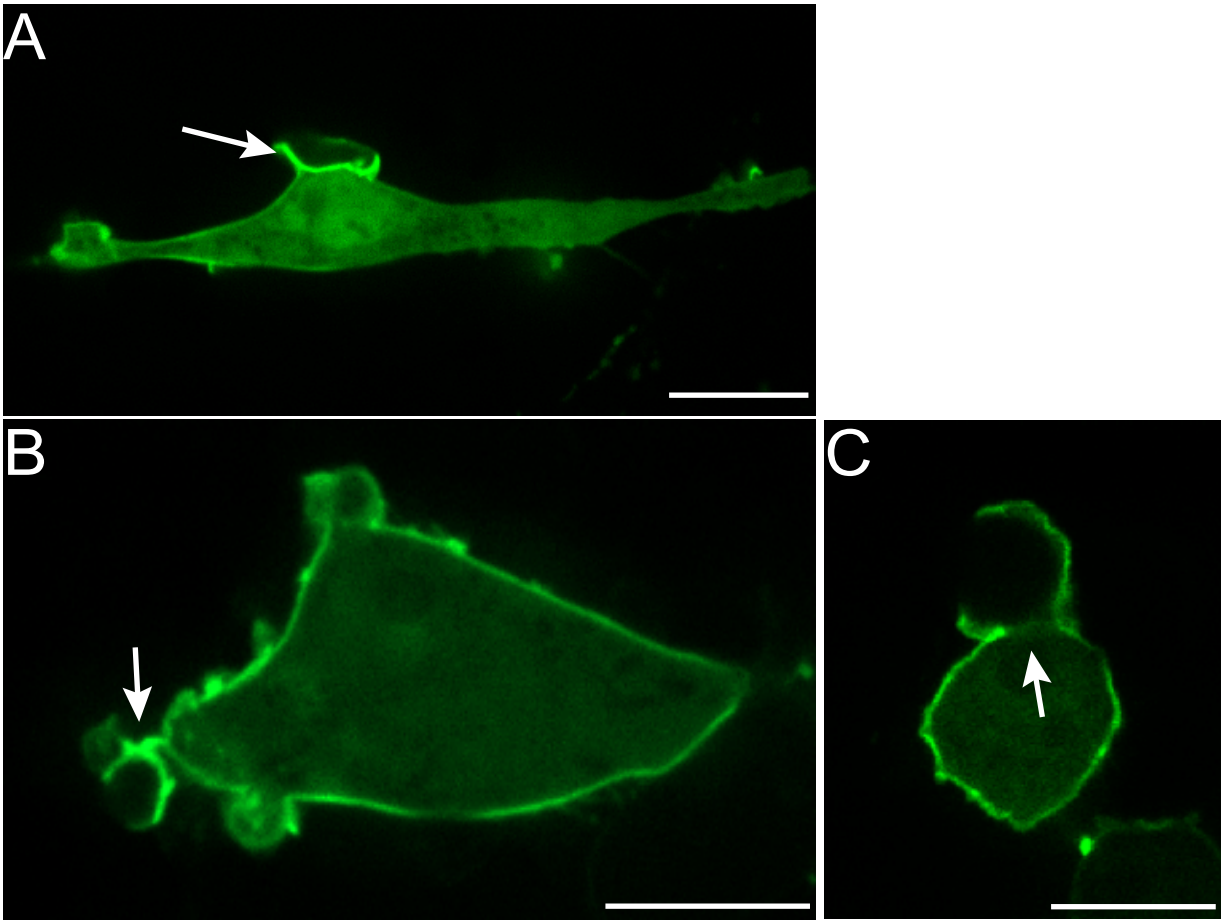

Figure S1. Changes in the free levels of PIP_2 and PIP_3 in forming phagosomes of J774 macrophages. (A) J774 macrophages expressing PH-AKT-GFP were incubated with IgG opsonized sheep red blood cells. PH-AKT-GFP accumulates at the nascent phagocytic cup (arrow), indicating PIP_3 accumulation. (B) J774 macrophages expressing PH-PLCδ-GFP were incubated with IgG opsonized 3 μm latex beads. Early stage nascent phagocytic cup (arrow) shows an accumulation of the PIP_2 probe. (C) J774 macrophages expressing PH-PLCδ-GFP were incubated with IgG opsonized 8 μm latex beads. Late stage phagocytic cup (arrow) shows a reduction in the membrane association of the PIP_2 probe at the base of the phagocytic cup, with the surrounding bulk plasma membrane maintaining constant PH-PLC δ-GFP staining. Scale bars = 10 μm.

Figure S2

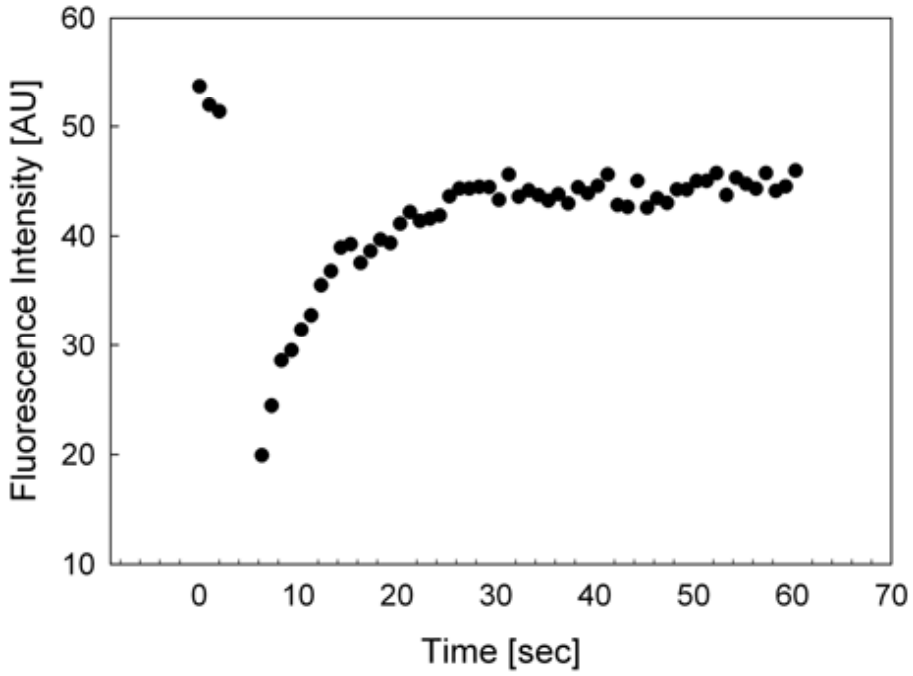

Figure S2. The fluorescence due to the lipid DiI exhibits a complete and rapid recovery after photobleaching the forming phagosome area. A macrophage injected with DiI C12 was allowed to engulf an IgG coated bead. The fluorescence was monitored prior to bleach in the phagosomal cup and followed after the bleach of the forming phagosome area, which took ~3 s. The time trace of the average fluorescence intensity per pixel in the ~ 20 μm^2 region of the forming phagosome had a recovery time of ~7 s: the recovery was essentially complete.

Figure S3

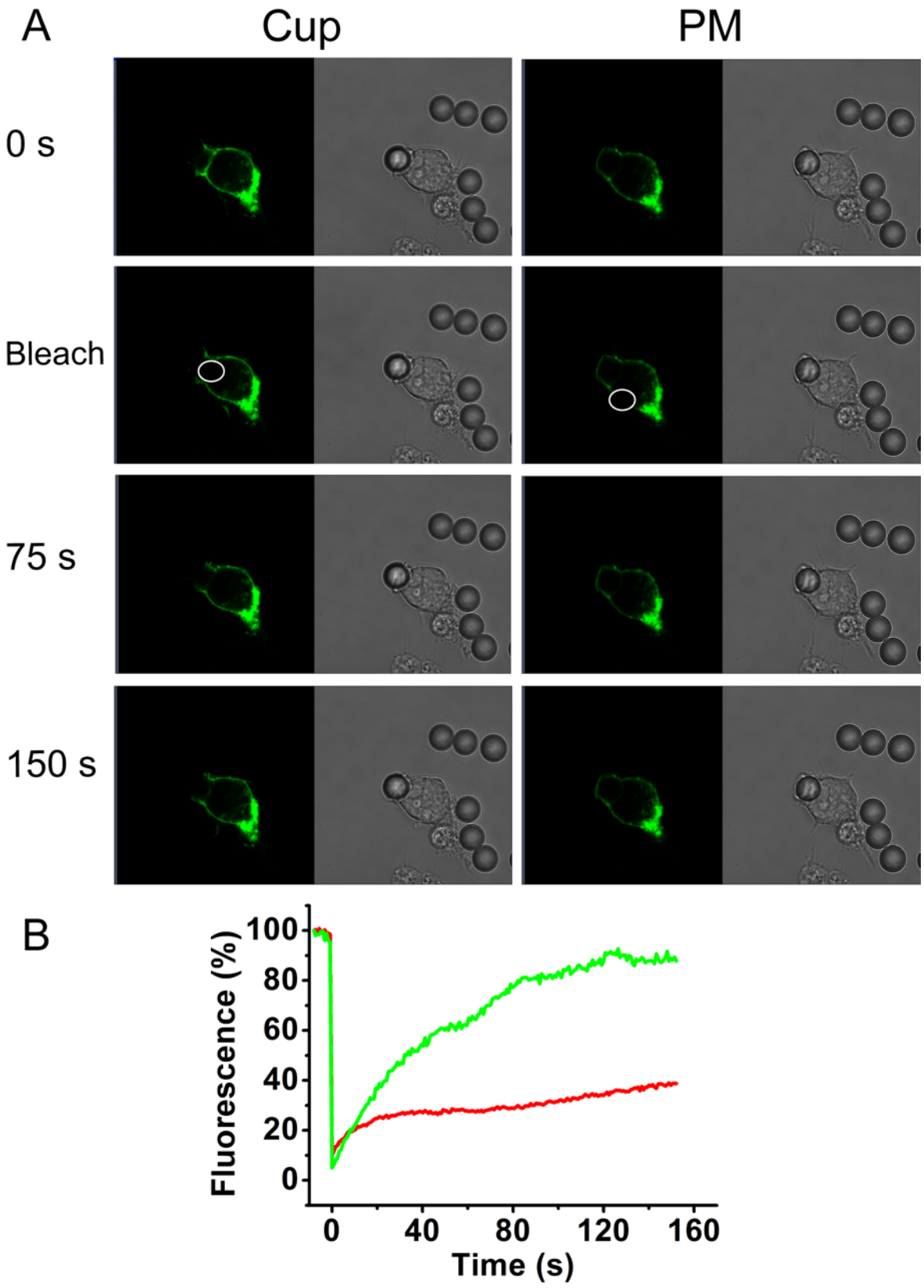
A
Cup
PM
0 s
Bleach
75 s
150 s
B
Fluorescence (%)
100
80
60
40
20
0
0
40
80
120
160
Time (s)

Fig. S3. Fluorescence recovery after bleach of PM-GFP in base of forming phagosome cup is much less than recovery from bulk of plasma membrane outside cup, which is essentially complete if this region is prebleached.

A We first bleached the region indicated by the white ellipse in the base of the cup (*Panel A: Cup*). The fluorescence increased ~30% in 100 s (with a recovery time of 10 s), as shown in panel B. We next prebleached then bleached the same area of plasma membrane outside the cup (*Panel A: PM)*, indicated by the white ellipse. The fluorescence recovered ~100% with a half time of ~ 50 s. For both the cup and PM images in panel A, the right hand panels show transmitted light images to indicate the location of the bead undergoing phagocytosis. Phagocytosis is essentially complete about 100 s after bleach of plasma membrane outside cup, and the bead was subsequently completely taken into the cell (not shown). T = 37 °C, RAW macrophages.

B) Fluorescence recovery curves corresponding to the cells shown in part A. Red, cup; green, PM.

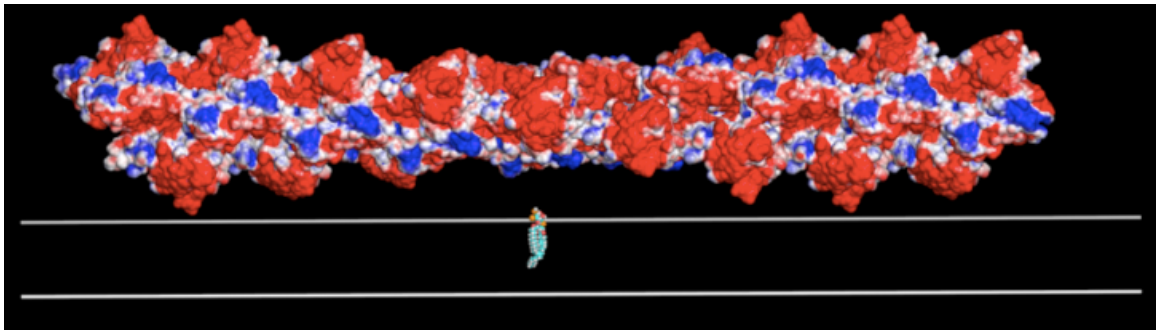

Figure S4. An actin filament adjacent to a membrane will not act as an electrostatic fence to impede PIP_2 diffusion. Molecular graphic view of a section of an actin filament (with electrostatic potential of -25 mV in red to +25 mV in blue on solvent-accessible surface representation), a PIP_2 (in space filling representation, and to scale with the actin), and the phosphate planes of the lipid bilayer (white lines). The electrostatic potential was calculated at 150 mM salt from the Poisson-Boltzmann equation using CHARMM-GUI *PBEQ-Solver* (www.charmm-gui.org/input/pbeqsolver). The closest point of the actin is ~0.5 nm from the phosphate plane. Langevin dynamics simulations show that while diffusion of PIP_2 is blocked in the regions of high negative electrostatic potential, the regions lined by positive charges form gaps allow relatively unrestricted diffusion of PIP_2 beneath the actin filament. These calculations suggest that actin filaments should ***not*** act as a 'fence' to greatly inhibit the diffusion of PIP_2 in the plasma membrane. Actin filaments close to the membrane could, however, sterically impede the diffusion of the larger PM-GFP, for which the cytoplasmic GFP protrusion is 3 nm wide by 4 nm high.

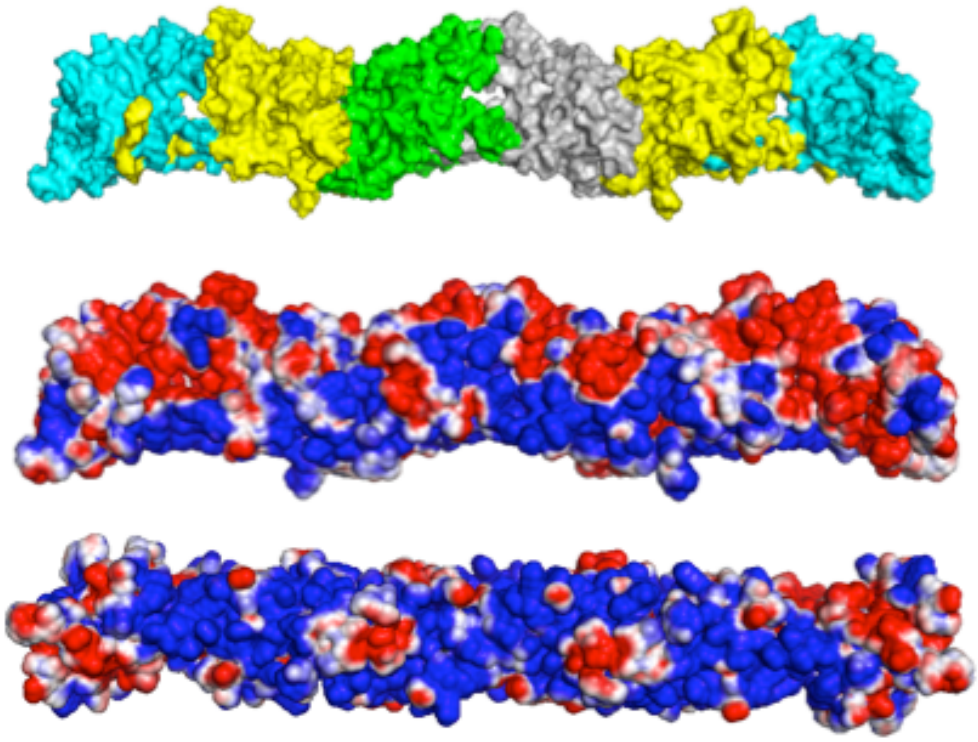

Figure S5. The septin filament has a positively charged face. Molecular graphics views of the hexameric unit of the human septin filament (PDB:2QAG). (top) Molecular surface representation with Septin-2 (*green* and *gray*), Septin-6 (*yellow*), and Septin-7 (*cyan*). This figure adapted from Sirajuddin et al. (2007): the C terminal extensions (not shown) protrude from the top of the figure. (middle) Solvent-accessible surface representation with electrostatic potential: -25 mV (*red*) and +25 mV (*blue*). (bottom). A view of a 90º rotation of the middle orientation, i.e., a view from the bottom of the middle figure.